Detection of Inlet Recirculation as an Early Indicator of Proximity to Instability in Centrifugal Compressors

ALASDAIR LOGAN, DAVID GARCIA
University of Strathclyde, Department of Mechanical and Aerospace Engineering, Glasgow, Scotland
alasdair.logan.2014@uni.strath.ac.uk and david.garcia@strath.ac.uk

GRZEGORZ LIŚKIEWICZ
Łódź University of Technology, Institute of Turbomachinery, Łódź, Poland
grzegorz.liskiewicz@p.lodz.pl

Compressing units are subject to a potentially damaging phenomenon known as surge at low flow rates. This effect may be preceded by an effect called inlet recirculation – a flow reversal upstream of the impeller. An experimental compressor rig was the basis of this investigation. High frequency pressure measurements were taken at a number of flow conditions and locations within the compressor. The measured signals were processed using Singular Spectrum Analysis (SSA), a nonparametric technique. SSA decomposes a signal into a number of Reconstructed Components (RCs), from which trends and oscillatory components may be extracted. The frequency spectra of each RC and their relative contributions to signal reconstruction were examined and comparison was made with spectral maps in existing literature. This study aimed to investigate SSA's ability to detect the presence of recirculation through analysis of a decomposed portion of a signal. The results demonstrated the potential of SSA to identify and extract oscillatory components with information about the local effect of inlet recirculation.

Keywords: Singular Spectrum Analysis, Inlet Recirculation, Compressor, Surge

1. Introduction

Centrifugal compressors are susceptible to unstable phenomena at low mass flow rates [1]. *Surge*, as discussed by Gravdahl and Egeland, is the most dangerous of these effects [2]. *Rotating stall* is also known to occur in centrifugal units, but its importance, according to De Jager [3], is questionable - this study aimed to identify a novel method of avoiding surge. Surge was first studied by Emmons [4], a mathematical model of surge in axial compressors was developed by Greitzer [5] and this was successfully applied to centrifugal units by Hansen [6]. Compressor performance reaches a maximum near and within the so-called surge margin; machine operation, however, must be controlled in this area in order to avoid potentially damaging vibration [2]. Botros and Henderson stated that any anti-surge system that limited operation based on a surge margin would induce a performance sacrifice, they went on to survey various proposed anti-surge systems to allow for operation within this margin [8]. These so-called *active* methods often deployed mechanical systems, such as valves or moveable vanes, to suppress surge [8, 9]. According to Gravdahl [10], the most promising of these methods was a close-coupled valve, as was proposed by Simon *et al* [11]. Fraser described inlet recirculation as a feature preceding surge in centrifugal compressors [12]. Hermez *et al* claimed that avoiding inlet recirculation could improve compressor efficiency [13]. Inlet recirculation has been detected in experimental studies as chaotic, high frequency drops in static pressure upstream of the impeller blade tip, combined with an increase in average pressure [14, 15]. This study attempted to use inlet recirculation as an indicator of surge inception. Previous studies had examined high frequency static pressure measurements taken at an experimental compressor rig at Łódź University of Technology, Poland [16]. These studies identified inlet recirculation as a region of high frequency oscillation in the frequency spectra at flow conditions preceding mild surge [17].

The data was analyzed using Singular Spectrum Analysis (SSA), a nonparametric modification of Principal Component Analysis for non-independent time series [18]. The 'caterpillar' method of SSA was used, as described by Golyandina *et al* [19]. This version of SSA emphasized the separability of the various Reconstructed Components (RCs) generated [20]. Initial uses of SSA were climatological and sociological, trends were extracted from time series of weather parameters by Ghil *et al* [21]. Mechanical applications of SSA have examined periodic vibration in complex dynamical systems [22]. This study added to work carried out by Garcia *et al*, where SSA was used to study static pressure measurements from a centrifugal compressor experiment [23, 24]. This work aimed to investigate the viability of condition monitoring based on SSA, through identification of the contribution of each RC to the reconstruction of the signal. It was hypothesized that inlet recirculation could be isolated and extracted with SSA.

2. Methodology

2.1. *Singular spectrum analysis*

SSA was performed according to the technique prescribed by Golyandina *et al* [19]. MATLAB was used to implement this technique, according to an algorithm developed by Alonso *et al* [25].This method was made up of the following four steps:

2.1.1. *Embedding*

The first step was the construction of the *trajectory* matrix through horizontal concatenation of a series of lagged vectors. These lagged vectors were derived from the original time series of static pressure measurements, $\boldsymbol{F} = [f_0, \ldots, f_{N-1}]$ according to the parameter L, *window length*. K lagged vectors were obtained, where $K = N - L + 1$. The following Hankel matrix, $\boldsymbol{X}$, was thereby obtained:

$$\boldsymbol{X} = \begin{bmatrix} f_0 & f_1 & f_2 & \cdots & f_{K-1} \\ f_1 & f_2 & f_3 & \cdots & f_K \\ f_2 & f_3 & f_4 & \cdots & f_{K+1} \\ \vdots & \vdots & \vdots & \ddots & \cdots \\ f_{L-1} & f_L & f_{L+1} & \cdots & f_{N-1} \end{bmatrix} \tag{1}$$

2.1.2. *Singular value decomposition*

Step 2 decomposed the trajectory matric, $\boldsymbol{X}$. Initially $\boldsymbol{X}$ was multiplied by its transpose, producing the matrix $\boldsymbol{S}$. Eigenvalues and their associated eigenvectors were extracted from $\boldsymbol{S}$. The square root of non-zero eigenvalues, λ_i, were ordered by magnitude and multiplied with their associated eigenvectors, $\boldsymbol{U_i}$, and $\boldsymbol{V_i}$, where $\boldsymbol{V_i = [X^T .\, U_i/\sqrt{\lambda_i}]^T}$, where the superscript T indicates matrix transposition. The products of these so-called *eigentriples*, were referred to as Principal Components (PCs), the sum of the PCs was a Singular Value Decomposition of the trajectory matrix. The creation of L PCs was the final stage of decomposition; reconstruction followed thereafter.

2.1.3. *Grouping*

The *grouping* stage of SSA selects PCs to be taken forward into step 4, *diagonal averaging*. Selection of PCs depends on the application. In this study the nature of the decomposition and the relationship between each component and physical flow features was of interest, therefore all L PCs were converted to reconstructed components (RCs). These RCs were then independently examined. It was hypothesized that an individual RC would be associated with inlet recirculation. An optimized SSA process would only subject this identified RC to diagonal averaging, but in this investigation all PCs were converted to RCs and studied. The window length was set to 50, in line with previous studies – the 50 RCs thus generated were to be analyzed. The ordering of PCs based on eigenvalues of the embedding matrix meant that the majority of the information making up the full signal was contained in the first two components – RCs 1 and 2 were the principal components of interest, as in Garcia *et al* [23].

2.1.4. *Diagonal averaging*

PCs were converted to vectors through *diagonal averaging*, creating Reconstructed Components, performed thus:

Let each PC be represented as a $L\,x\,K$ matrix with elements y_{ij}, $1 \le i \le L_w, 1 \le j \le K$. Let $L^* = min(L_w,K)$, $K^* = max(L,K)$. Let $y_{ij}^* = y_{ij}$ *if* $L < K$, otherwise let $y_{ij}^* = y_{ji}$. PCs were converted to RCs $(g_0,\dots, g_{N-1})$ by the formulae:

$$g_k = \begin{cases} \dfrac{1}{k+1}\displaystyle\sum_{m=1}^{k+1} y^*_{m,k-m+2} & \text{for } 0 \le k \le L^* - 1 \\ \dfrac{1}{L^*}\displaystyle\sum_{m=1}^{L^*} y^*_{m,k-m+2} & \text{for } L^* \le k < K^* \\ \dfrac{1}{N-k}\displaystyle\sum_{m=1}^{L^*} y^*_{m,k-m+2} & \text{for } K^* \le k < N \end{cases} \tag{2}$$

Each RC obtained in this way may be summed to reconstruct the signal to the required resolution. In this investigation the RCs generated were independently studied, as discussed above – this summing process was not performed.

2.2. ***Experimental rig***

SSA was used to analyse signals obtained from an experimental centrifugal compressor, as described hereafter. Experiments were performed on a single-stage centrifugal compressor, as described by Liśkiewicz *et al* [16] and Garcia *et al* [23, 24]. These authors described the geometry of the experimental rig in detail. A half cross-section is presented in Figure 1. Ambient flow entered the compressor through inlet pipe **A**. Then it was accelerated through the Witoszynski nozzle **B** and onwards to the impeller **C**. A constant gap of δ = 0.8 mm was maintained between impeller blade tips and the shroud, along length L – this was considered a critical feature with respect to inlet recirculation. A vanless diffuser, **D**, followed the impeller. Finally, the flow entered the circular volute, **E**, where an initially rectangular cross section expanded to a circular outlet.

The rotor was driven by an asynchrous AC motor and rotated at f_{rot} = 100 Hz. The impeller blade tip passing frequency was f_{BP} = 2.3 kHz. A throttling valve at the outlet allowed for flow rate control, this was quantified by the Throttle Opening Area (TOA), expressed as a percentage. Measurements were taken at 1% increments of TOA, with a settling time of 20s included to eliminate transient phenomena associated with throttling.

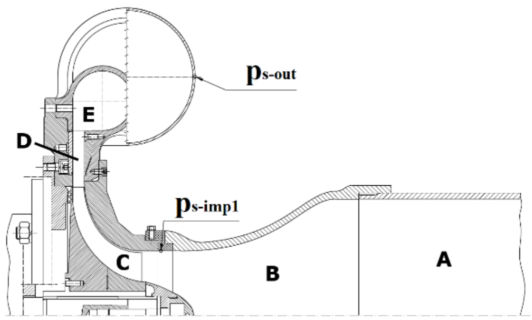

Fig. 1. Cross section of experimental rig with relevant pressure transducer locations

Subminiature Kulite transducers were used to measure static and total pressures of the flow at various points. Figure 1 shows the arrangement of these transducers. Sensor $p_{s\text{-}imp1}$ was of particular interest, as it was upstream of the impeller tip, where recirculatory flow was detected [16]. Outlet measurements, at $p_{s\text{-}out}$, where the local phenomenon of inlet recirculation was absent, were used as a control. Each sensor gathered 2^{21} samples at each TOA increment, with a sampling frequency of f_s = 100 kHz.

2.3. *Reconstructed components frequency spectra*

The frequency spectra of individual RCs were obtained by a Fourier transform; this study examined the frequency domain behaviour of the various components obtained by the SSA decomposition. Parallel plots of a range of RCs were generated in order to elucidate the nature of the decomposition. *Spectral maps* were generated, according to a plotting technique used by Liśkiewicz *et al* in a study of the original signal [16]. Comparison between these previous plots and decomposed portions of the full signal were used to analyse the relationship between each RC and compressor instability. Finally, a more precise range of TOAs were examined to fortify claims made regarding the selection of a particular RC as an indicator of the onset of inlet recirculation.

3. Results

3.1. *Signal decomposition*

The behavior of the SSA decomposition was the initial subject of investigation. The frequency spectra of the first ten RCs were plotted in order to outline the relative contribution of each component to the signal reconstruction. It was expected that a single RC could be related to inlet recirculation such that a fraction of the full signal could provide an indication of the onset of inlet recirculation and subsequent unstable phenomena. These investigations were focused on a throttle position within the region of inlet recirculation, TOA = 22% was chosen as the pressure oscillation representative of this feature was here most prominent.

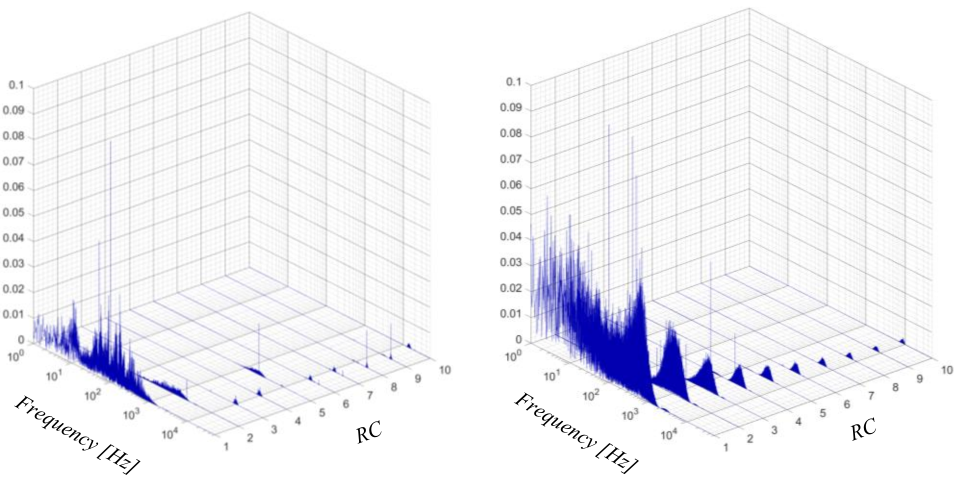

(a) $p_{s\text{-}out}$ (b) $p_{s\text{-}imp1}$

Fig. 2. Frequency Sp RCs 1-10, TOA = 22%.

Figure 2 shows the plots thus created. Th ots demonstrated the local character of inlet recirculation, manifest as increased ampli ›scillation at the higher part of the frequency spectra. The decomposition at $p_{s\text{-}out}$ shov ›v RC 1 dominated the reconstruction, with the majority of 'information' in the original signal – here captured as the extent and density of the RC frequency spectrum – contained within the first component. This was a result of the ordering of RCs based on eigenvalues obtained from the embedding matrix [19].

The importance, however, of RC 1 did not seem as prominent at $p_{s\text{-}imp1}$ where RCs 2 and above appeared to offer more to the reconstruction. These RCs displayed a clear relationship with frequency, with higher frequencies within the original time series captured by successive RCs, with an associated decrease in magnitude. These frequency spectra seemed to fall within the region identified by Liśkiewicz *et al* as being indicative of inlet recirculation [16]. RC 1 also captured some of this region, but it was obscured by other information within this component, such as the blade rotation frequency, f_{rot} = 100 Hz. The blade passing frequency, f_{BP} = 2.3 kHz, was seen as a peak in RC 3 - this clearly demonstrated the ability of SSA to isolate particular flow features. Inlet recirculation, however, appeared to be reconstructed by a combination of RCs, including RC 1. 50 RCs were generated, as determined by the choice of window length. Inspection of Figure 2 emphasized the minimal contribution of higher RCs and it was, therefore, not thought necessary to investigate the remaining 40 RCs. Inclusion of all generated RCs was thought to compromise the fidelity of the portrayal of the first two, where the majority of relevant information was contained. RCs 1 and 2 thus became the focus of the remainder of this investigation.

3.2. *Spectral maps*

Further graphical representation of the signal decomposition followed a technique adopted by Liskiewicz *et al* – the creation of *spectral maps* where a range of TOAs were simultaneously plotted for individual RCs. A logarithmic pressure amplitude scale and a frequency limit of 1 Hz – 50000 Hz were replicated in these plot in order to encourage a more valuable comparison process. Throttle position was limited from 5% < TOA < 40% in this study, where instability at low flow rates was of particular interest. The computational demand induced by the abundance of data plotted was tempered by limiting the signal length to 1 million samples – such a limitation did not produce any divergence with the full signal plotted by Liśkiewicz *et al* [16].

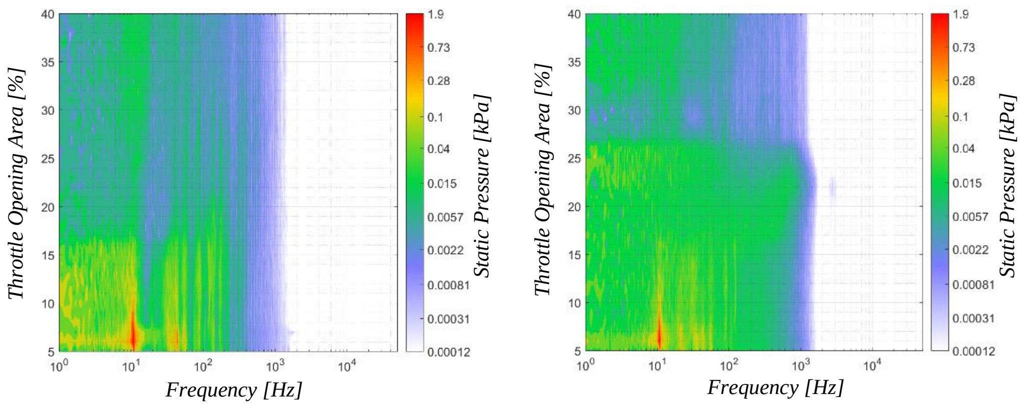

(a) $p_{s\text{-}out}$ (b) $p_{s\text{-}imp1}$

Fig. 3. Spectral maps of RC 1, 5% < TOA < 40%.

Figure 3 is made up of spectral maps generated at the outlet and upstream of the impeller shroud, $p_{s\text{-}imp1}$, for RC 1. This component, as explained above, contained the majority of the information in the original signal and as such these plots were most similar to those generated by Liśkiewicz *et al*. This similarity justified such a plotting technique. There was a significant failure in RC 1 to replicate frequencies greater than 1000 Hz – this area of the original spectral map was expected to be replicated by RCs 2 and higher. The appearance of deep surge, manifest as a frequency peak at 10.8 Hz at lower TOAs was seen at both sensor locations – this confirmed the global character of deep surge. This frequency was approximately predicted by calculation of the Helmholtz frequency, f_H = 11.5 Hz by Liśkiewicz *et al*, where the internal volume of the experimental compressor rig was treated as a Helmholtz resonator. This technique for predicting the resonance at deep surge was suggested by Fink *et al* [26] and appeared to provide a reasonable approximation of the resonant frequency.

The principal feature of interest was inlet recirculation, expected to appear solely in Figure 4(b). This phenomenon was identified as an area of high frequency (~1000 Hz) pressure oscillation at 17% < TOA < 27%. It had been established from Figure 2 that inlet recirculation was partially captured by RC 1, and this was confirmed through inspection of Figure 3(b). No such region was seen at the outlet, where some indication of instability appeared at TOA = 17%: this was attributed to mild surge. Comparison with Liśkiewicz *et al* [16], however, showed that the limitation of RC 1 to capture higher frequencies meant that much of the area identified as being indicative of inlet recirculation was absent; it was thought this would be captured by RC 2, captured below as Figure 4.

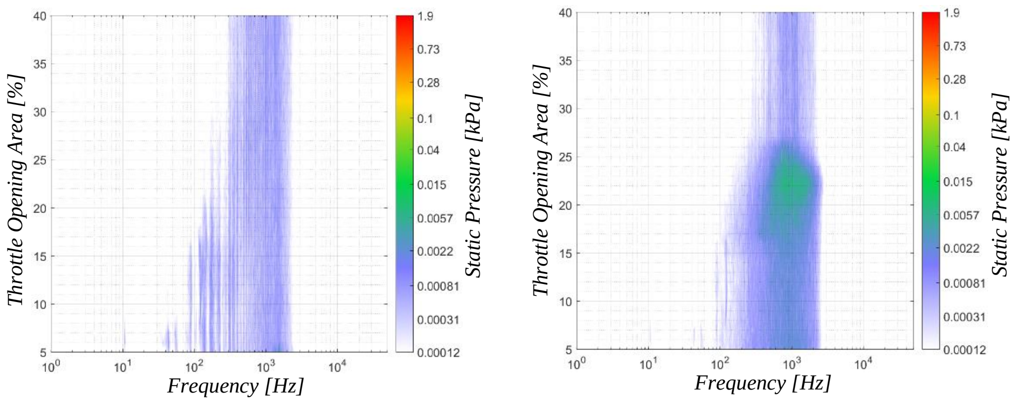

(a) $p_{s\text{-}out}$ (b) $p_{s\text{-}imp1}$

Fig. 4: Spectral maps of RC 2, 5% < TOA < 40%.

Figure 4 shows RC 2 subjected to the spectral map plotting method. The logarithmic color bar allowed RC 2 to be represented at the same scale as RC 1, but the great difference in magnitude should be noted. The appearance of inlet recirculation at TOA = 26% was clear in Figure 4(b) – this was later than was seen in RC 1. It could be suggested that RC 1 captured inlet recirculation at a higher TOA due to the pressure oscillation at the onset of this feature occurring within the range of frequencies generally captured by RC 1. As this feature increased in prominence it was manifest as a broader band in the frequency spectra and RC 2 was required to reproduce this oscillation. Again there was some instability appearing within the region of mild surge at $p_{s\text{-}out}$, but no indication of inlet recirculation, as was expected.

3.3. *Further analysis of reconstructed component 2 (RC 2)*

A more detailed examination of RC 2 was demanded, given the promising results of the examination of the spectral maps. These maps proved the ability of SSA to reproduce flow features seen in the original signal; further understanding of the behavior of RC 2 was required if this component was to be the basis of a control system. Figure 5 shows this component in detail, with a more selective choice of throttle positions, 15% < TOA < 30% - the emphasis of this study was now entirely focused on inlet recirculation. The stability of RC 2 at $p_{s\text{-}out}$ was clear, as well as its ability to clearly show the onset of flow recirculation at $p_{s\text{-}imp1}$. Inlet recirculation was of maximum prominence at TOA = 22%, this justified the particular examination of this throttle position in 3.1.

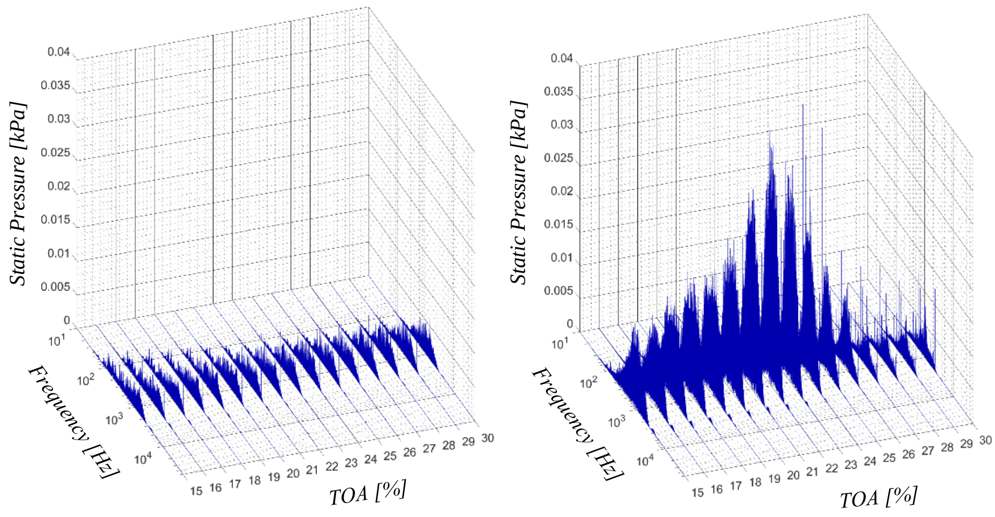

(a) $p_{s\text{-}out}$ (b) $p_{s\text{-}imp1}$

Fig. 5. Frequency Spectra of RC 2, 15% < TOA < 30%

The potential of SSA in this application was now clear. It was now be suggested that the decomposition of the signal by SSA could produce a component that gave a clear indication of the onset of inlet recirculation. RC 2 isolated inlet recirculation from the information describing other flow features, contained in RC 1. It was thus possible to diagnose this phenomenon by examination of a fraction of the original signal.

4. Conclusions

4.1. *Outcomes*

This study has enhanced the understanding of Singular Spectrum Analysis as a technique for condition monitoring of compressors, based on high frequency static pressure measurement. A system for surge avoidance can be theorised, based on detection of the presence of a local phenomenon preceding surge – inlet recirculation. Previous work had generated performance curves for this system which suggest maximum pressure ratio is obtained in the area immediately preceding inlet recirculation [23] – condition monitoring based on this phenomenon should ensure consistent operation in this region, where performance and stability are optimal.

Inlet recirculation can be isolated from a pressure signal using SSA, a time series analysis tool. SSA can decompose and reconstruct a signal based on the selection of a number of RCs, ordered according to their relative contribution to the reconstruction of the original signal. These RCs can be isolated and associated with physical phenomena, allowing an appropriate fraction of the full signal to capture the appearance of inlet recirculation. The results showed RC 2 was the best choice for such a system due to the clarity with which it indicated the onset of inlet recirculation.

4.2. *Future work*

RC 2 was confirmed as a potential indicator of inlet recirculation; a number of suggestions can now be made regarding the implementation of SSA in this field. Window length was held constant in this study, following the methodology of previous authors [23, 24], modification of this parameter could be the subject of future investigations. Leles *et al* showed that an increased window length resulted in greater so-called *separability*: the ability of SSA to separate the frequency spectrum of the original signal into increasingly shorter sections [27]. A potential study into window length variation could attempt to more precisely extract particular features by increasing this parameter.

Implementation of the result of this study would involve the development of a control system based on an SSA decomposition of the original signal. This could involve the individual extraction of RC 2, rather than all 50 RCs. The obtained signal could potentially be compared to some reference signal at TOA = 30% by correlation analysis or setting a maximum RMS value. In this way a diagnosis of inlet recirculation could be made and surge would be avoided by supplying this information to some mechanical flow regulation device, as surveyed by Botros and Henderson [7].

Acknowledgement

This work was funded by the Polish National Centre for Research and Development (Grant No. Lider/447/L-6/14/NCBR/2015).

References

[1] **Bloch, H.**: *A Practical Guide to Compressor Technology*, Wiley-Interscience, Hoboken, **2006.**

[2] **Gravdahl, J.T. and Egeland O.**: *Compressor Surge and Stall – Modelling and Control*, Springer, London, **1999.**

[3] **De Jager, B.**: Rotating stall and surge control: a survey, *Proc. 34th. IEEE Conference on Dec. and Con. Vol. 2,* 1857-1862, **1995**.

[4] **Emmons, H.W., Pearson C.E. and Grant H.P.**: Compressor surge and stall propagation, *Trans. ASME*, **77**(4), 455-469, **1955**.

[5] **Greitzer, E.M.**: Surge and rotating stall in axial flow compressors, Part i: Theoretical compression system model. *Jo. Eng. Power,* **98**(2), 190-198, **1976**.

[6] **Hansen, K.E., Jorgensen, P. and Larsen P.S.**: Experimental and theoretical study of surge in a small centrifugal compressor, *J Fluids Eng,* **107**, 391-395, **1981.**

[7] **Botros, K.K. and Henderson, J.**: Developments in centrifugal compressor surge control – a technology assessment, *J Turbomach,* **116**(2), 240-249, **1994**.

[8] **Epstein, A.H., Ffowcs Williams, J.E. and Greitzer, E.M.**: Active suppression of aerodynamic instabilities in turbomachines, *J. Propul. Power*, **5**(2), 204-211, **1989**.

[9] **Pinsley, F.E., Guenette, G.R., Epstein, A.H. and Greitzer, E.M.**: Active stabilization of centrifugal compressor surge, *J Turbomach*, **113**(4), 723-732, **1991**.

[10] **Gravdahl, J.T.**: *Modeling and control of surge and rotating stall in compressors,* Ph. D. Thesis, Norwegian University of Science and Technology, **1998**.

[11] **Simon, J.S., Valavani, L., Epstein, A.H. and Greitzer, E.M.**: Evaluation of approaches to active compressor surge stabilization, *J Turbomach,* **115**, 57-67, **1993**.

[12] **Fraser, W.H.**: Flow recirculation in centrifugal pumps, *Construct. Fluid Mach. Relat. Des. Perform.,*312-320, **1981**.

[13] **Hermez, Y.M. *et al***: Comparison of inlet curved disk arrangement for suppression of recirculation in centrifugal pump impellers, *Proc. of the ASME 2016 Mech. Congress*, Phoenix, **2016**.

[14] **Mizuki, S. and Oosawa, Y**.: Unsteady flow within centrifugal compressor channels under rotating stall and surge, *J Turbomach*, **114**(2), 312-320, **1992**.

[15] **Tamaki, H.**: Experimental study on surge inception in a centrifugal compressor, *J. Fluid Mach. Syst.*, **2**(4), 409-417, **2009**.

[16] **Liśkiewicz, G. *et al***: Identification of phenomena preceding blower surge by means of pressure spectral maps, *Exp. Therm. Fluid. Sci.*, **54**, 267-278, **2014**.

[17] **Liśkiewicz, G. and Horodko, L**.: Time-frequency analysis of the surge onset in the centrifugal blower, *Open Eng.*, **5**(1), 299-306, **2015**.

[18] **Hassani, H**.: Singular spectrum analysis: methodology and comparison, *J. Data Sci.*, **5**, 239-257, **2007**.

[19] **Golyandina, N., Nekrutkin, V. and Zhigiljavsky A**.: *Analysis of Time Series Structures: SSA and Related Techniques*, Chapman & Hall CRC, Boca Raton **2001**.

[20] **Polukoshko, S., Hilkevica, G. and Gonca, V.:** Nonstationary processes studying based on "caterpillar" – SSA method, *Vib. Eng. Tech. Mach. Mech. Mach. Sci.*, **23**, 999-1008, **2015**.

[21] **Ghil, M. et al**. Advanced spectral methods for climatic time series, *Rev Geophys.*, **40**(1), 3-41, **2002.**

[22] **Pasamanter, R**.: Variational search of periodic motions in complex dynamical systems, *Chaos, Solitons Fractals*, **6**, 447-454, **1995**.

[23] **Garcia, D., Stickland, M. and Liśkiewicz, G.:** Dynamical system analysis of unstable flow phenomena in centrifugal blower, *Open Eng.*, **5**(1), 332-342, **2015**.

[24] **Garcia, D. and Liśkiewicz, G**.: Stable or not stable? Recognizing surge based on the pressure signal, *Trans. Ins. Fluid-Flow Mach.*, **133**, 55-68, **2016.**

[25] **Alonso, F.J., Del Castillo, J.M. and Pintado, P**.: Application of singular spectrum analysis to the smoothing of raw kinematic signals, *J. Biomech.*, **38**, 1085-1092, **2005**.

[26] **Fink, D.A., Cumpsty, N.A. and Greitzer E.M.**: Surge dynamics in a free-spool centrifugal compressor system, *J. Turbomach.*, **114**(2), 321-332, **1992**.

[27] **Leles, M.C.R. et al** : Frequency-domain characterization of singular spectrum analysis eigenvectors, *Proc. of IEEE Symp. Sig. Process. and IT*, Limassol, Cyprus, **2016**.